THE CONTRIBUTION OF EUV FROM CLUSTERS OF GALAXIES TO THE COSMIC IONIZING BACKGROUND

SCOTT W. RANDALL AND CRAIG L. SARAZIN
Department of Astronomy, University of Virginia, P. O. Box 3818, Charlottesville, VA 22903-0818;
swr3p@virginia.edu, cls7i@virginia.edu
Astrophysical Journal, in press

ABSTRACT

Recent observations with the Extreme Ultraviolet Explorer (EUVE) suggest that at least some clusters of galaxies are luminous sources of extreme ultraviolet (EUV) radiation. It is not clear yet whether EUV emission is a general feature of clusters; for the purposes of limiting the contribution to the background radiation, we assume that it is true of most clusters. Assuming that the source of the EUV emission is inverse Compton (IC) scattering of the Cosmic Microwave Background photons by relativistic electrons, we construct a simple model for the expected average emission from clusters as a function of their mass and the redshift of interest. Press-Schechter theory is used to determine the abundance of clusters of various masses as a function of redshift. We determine the amount of background radiation produced by clusters. The total mean intensity, spectrum, and the ionization rates for H I and He II are determined at present and at a variety of redshifts. Because clusters form by the merger of smaller subclusters, the amount of EUV background radiation should be larger at present than in the past. We compare our results to the ionizing background expected from quasars. We find that while clusters do contribute a significant EUV background, it is less than a percent of that expected from quasars.

Subject headings: cosmic rays — diffuse radiation — galaxies: clusters: general — intergalactic medium — large-scale structure of the universe — ultraviolet: general

1. INTRODUCTION

Recently, extreme ultraviolet (EUV) and very soft Xray emission has been detected from a number of clusters of galaxies. Except for the Coma and Virgo cluster (Bowyer, Lampton, & Lieu 1996; Lieu et al. 1996a,b,c; Bowyer, Berghöfer, & Korpela 1999; Berghöfer, Bowyer, & Korpela 2000), the individual detections are controversial. Other clusters which may have been detected include Abell 1795 and Abell 2199 (Bowyer, Lieu, & Mittaz 1998; Mittaz, Lieu, & Lockman 1998), Abell 4038 (Bowyer et al. 1998), and Abell 4059 (Bowver 2000). The excess EUV detections in the rich clusters (i.e., not Virgo) correspond to luminosities of $\sim 10^{44} {\rm ergs \ s^{-1}}$. The detections of Abell 1795 and Abell 2199 as extended EUV sources have been quite controversial. For both clusters, detections with EUVE were claimed by Bowyer et al. (1998) and Mittaz et al. (1998). However, Bowyer, Berghöfer, & Korpela (1999) argued these detections were due to an incorrect subtraction of the background. In Abell 2199, Lieu et al. (1999b) reobserved the cluster, and continue to claim detection of an extended EUV source. An associated soft X-ray excess may have been seen with BeppoSAX (Kaastra et al. 1999). Recently, XMM appears to have confirmed the presence of very extended, EUV/soft-X-ray excess emission in Abell 1795 (Arnaud 2000). In addition to the controversies about individual clusters, Arabadjis & Bregman (1999) argue that all the detections may be due to uncertainties in Galactic absorption.

Thus, it is not certain at this point whether excess EUV emission is a general characteristic of clusters of galaxies. In order to limit the contribution of cluster EUV emission to the extragalactic background, we will assume that it is, in fact, a general property of rich clusters. If this is the case, then our calculations may give a determination of

the cluster contribution to the EUV background. If EUV excess emission is present in only a fraction of rich clusters, then our calculations will give a strong upper limit to the contribution to the extragalactic background.

A promising theory for the EUV emission by clusters is that it is produced by inverse Compton (IC) scattering of the Cosmic Microwave Background (CMB) by relativistic electrons in the intracluster medium (Hwang 1997; Bowyer & Berghöfer 1998; Enßlin & Biermann 1998; Sarazin & Lieu 1998). This requires the presence of a distinct population of relatively low energy relativistic electrons with energies of ~100 MeV (Bowyer & Berghöfer 1998) beyond the population of higher energy electrons which produce radio emission in a small fraction of clusters (e.g., Feretti 1999). Such a distinct population is expected theoretically, because the lower energy electrons have lifetime which are comparable to the Hubble time, while the radio emitting electrons have very short lifetimes (Sarazin 1999; Atoyan & Völk 2000; Takizawa & Naito 2000).

An alternative theory is that the EUV emission is thermal in origin (Mittaz et al. 1998; Lieu, Bonamente, & Mittaz 1999a). There are a number of concerns with this thermal model, particularly with the energetics (Fabian 1996; Sarazin & Lieu 1998). Recently, Lieu et al. (1999a) have argued that the observed EUV to soft X-ray spectra of clusters decline rapidly with increasing frequency, and that this favors a thermal model. However, such a rapid decline is, in fact, what was predicted by the IC model (Sarazin & Lieu 1998; Sarazin 1999; Atoyan & Völk 2000; Takizawa & Naito 2000; Figure 3 below).

In any case, we will normalize our calculations of the EUV emission from clusters to the observed EUV flux from the Coma cluster, which is the best observed rich cluster. Thus, our results are somewhat independent of the emis-

sion mechanism for the EUV emission. In detail, we need a model to scale the EUV luminosity of Coma to other clusters and other redshifts, and we need a model for the spectrum of the emission. At present, there are no detailed thermal models for the EUV emission from clusters which provide such predictions. On the other hand, the IC model provides a very simple scaling of the luminosity and spectrum to other masses of clusters and to other redshifts (§ 3 below). Thus, we will adopt the IC model for the emission to scale the observed flux of the Coma cluster to other clusters and redshifts.

If this radiation really is a common feature of clusters at the indicated luminosity levels, it might make a contribution to the intergalactic background radiation field at UV through soft X-ray energies. In this paper, we estimate the mean intensity of the diffuse EUV background from galaxy clusters, both at the current epoch and at higher redshifts. We will compare the radiation field from clusters with that produced by quasars and other active galactic nuclei (AGN) (e.g., Haardt & Madau 1996). In § 2, we use Press-Schechter (1974) theory to calculate the abundance of clusters of a given mass as a function of redshift. In § 3, the EUV emission of clusters of a given mass is calculated, based on a simple IC theory. We assume that both the thermal energy of the intracluster gas and the energy of relativistic electrons are produced ultimately by intracluster shocks, and that these shocks convert a fixed fraction of the shock energy into relativistic particles. The resulting diffuse radiation field at the present epoch and at higher redshifts are given in § 4. The resulting ionization rates of H I and He II are also derived there. The cluster diffuse EUV is compared to that produced by guasars and other AGN. The conclusions are summarized in § 5.

2. MASS DISTRIBUTION OF CLUSTERS

2.1. Predicted Mass Distribution of Clusters

In order to determine the total background radiation from galaxy clusters, it is first necessary to model their number density and its evolution with redshift z. While the present-day abundance of rich clusters is welldetermined from observations (see § 2.2 below), the evolution of the cluster abundance is poorly determined at present, particularly at high redshifts. Thus, we will use the Press-Schechter (PS) formalism (Press & Schechter 1974) to model the cluster density and its evolution, with parameters chosen to fit the observed present-day properties of clusters and the results of more detailed numerical models of large-scale structure. Comparisons to observations of clusters and to numerical simulations show that the PS provides an excellent representation of the statistical properties of clusters, if the PS parameters are carefully selected (e.g., Lacey & Cole 1993; Bryan & Norman 1998; Viana & Liddle 1999). Let n(M,z)dM be the comoving number density of clusters with masses in the range M to M + dM in the Universe at a redshift of z. According to PS, this differential number density is given by

$$n(M,z) dM = \sqrt{\frac{2}{\pi}} \frac{\overline{\rho}}{M^2} \frac{\delta_c(z)}{\sigma(M)} \left| \frac{d \ln \sigma(M)}{d \ln M} \right|$$

$$\times \exp \left[-\frac{\delta_c^2(z)}{2\sigma^2(M)} \right] dM, \qquad (1)$$

where $\overline{\rho}$ is the current mean density of the Universe, $\sigma(M)$ is the current rms density fluctuation within a sphere of mean mass M, and $\delta_c(t)$ is the critical linear overdensity for a region to collapse. In using this expression, we have made the usual assumptions that each cluster under consideration has recently collapsed $(z_{obs} \approx z_{coll})$ and that collapse is spherically symmetric. However, comparisons to numerical simulations show that this expression gives a good fit to the detailed results if the parameters are selected carefully (e.g., Lacey & Cole 1993; Viana & Liddle 1999). We will assume a power-law spectrum of density perturbations, which is consistent with CDM models:

$$\sigma(M) = \sigma_8 \left(\frac{M}{M_8}\right)^{-\alpha}, \qquad (2)$$

where σ_8 is the present day rms density fluctuation on a scale of 8 h^{-1} Mpc, $M_8 = (4\pi/3)(8\,h^{-1}\,\mathrm{Mpc})^3\bar{\rho}$ is the mass contained in a sphere of radius 8 h^{-1} Mpc, and the Hubble constant is $H_0 = 100\,h\,\mathrm{km\ s^{-1}\ Mpc^{-1}}$. The exponent α is given by $\alpha = \frac{n+3}{6}$, where the power spectrum of fluctuations varies with wavenumber k as k^n ; we assume n = -7/5, which leads to $\alpha = 4/15$ throughout. Using the above relations, we can rewrite equation (1) as

$$n(M,z) dM = \sqrt{\frac{2}{\pi}} \frac{\overline{\rho}}{M^2} \frac{\delta_c(z)}{\sigma(M)} |\alpha|$$

$$\times \exp\left[-\frac{\delta_c(z)^2}{2\sigma^2}\right] dM.$$
 (3)

The normalization of the power spectrum and overall abundance of clusters is set by σ_8 . Although there are published values for this constant (e.g., Viana & Liddle 1999; Bahcall & Fan 1998), we choose to normalize our calculations to a fixed value for the observed local abundance of clusters. Specifically, for each cosmology, we choose the value of σ_8 such that the present day integrated number density of clusters with mass $M>8\times 10^{14}\,h^{-1}\,M_{\odot}$ matches the observed value of $2\times 10^{-7}\,h^3$ Mpc⁻³ (Bahcall & Fan 1998). This method has the advantage that it forces the present day cluster abundance to be the same for each cosmology, as opposed to having a small spread in values, which occurs if an analytic approximation for the variation of σ_8 with cosmology is used.

The cosmological model is characterized by several parameters. The dependence on the Hubble constant $H_0=100\,h$ km s⁻¹ Mpc⁻¹ just produces an overall scaling of the results, which we include through the factor h. We characterize the cosmological solution by the two standard dimensionless parameters. First, $\Omega_0 \equiv \bar{\rho}/\rho_c$ is the ratio of the current mass density to the critical mass density $\rho_c = 3H_0^2/(8\pi G)$. Second, $\Omega_\Lambda \equiv \Lambda/(3H_0^2)$, where Λ is the cosmological constant. We will consider three distinct cosmological models in our analysis: an Einstein-deSitter universe ($\Omega_0=1,\ \Omega_\Lambda=0$), an open universe ($\Omega_0=0.3,\ \Omega_\Lambda=0$), and a low-density flat universe ($\Omega_0=0.3,\ \Omega_\Lambda=0.7$). The number density of clusters evolves differently in each of these three models. While the latter two models agree better with observations (e.g., Bahcall & Fan 1998), we include the closed model for completeness.

The evolution of the density of clusters is encapsulated in the $\delta_c(z)$ term in equation (3). In general, $\delta_c(z) \propto D(t)$, where D(t) is the growth factor of linear perturbations as

a function of cosmic time t (see Peebles [1980], § 11 for details). Expressions for the $\delta_c(z)$ in different cosmological models are:

$$\delta_c(z) = \begin{cases} \frac{3}{2} D(t_0) \left[1 + \left(\frac{t_{\Omega}}{t} \right)^{\frac{2}{3}} \right] \\ \frac{3(12\pi)^{\frac{2}{3}}}{20} \left(\frac{t_0}{t} \right)^{\frac{2}{3}} \\ \frac{D(t_0)}{D(t)} \left(\frac{3(12\pi)^{\frac{2}{3}}}{20} \right) (1 + 0.0123 \log_{10} \Omega_f) \end{cases}$$
(4)

for the open, closed, and flat models respectively. For the open model ($\Omega_0 < 1$, $\Omega_{\Lambda} = 0$), $t_{\Omega} \equiv \pi H_0^{-1} \Omega_0 (1 - \Omega_0)^{-\frac{3}{2}}$ represents the epoch at which a nearly constant expansion takes over and no new clustering can occur, and the growth factor can be expressed as

$$D(t) = \frac{3 \sinh \eta \left(\sinh \eta - \eta\right)}{\left(\cosh \eta - 1\right)^2} - 2 \tag{5}$$

where η is the standard parameter in the cosmic expansion equations (Peebles 1980, eqn. 13.10)

$$\frac{1}{1+z} = \frac{\Omega_0}{2(1-\Omega_0)} \left(\cosh \eta - 1\right) ,
H_0 t = \frac{\Omega_0}{2(1-\Omega_0)^{\frac{3}{2}}} \left(\sinh \eta - \eta\right) .$$
(6)

The solution for δ_c in the Einstein-deSitter model can be obtained from the open model solution by the limit $t_{\Omega}/t \to \infty$ (Lacey & Cole 1993). To evaluate δ_c in the flat model $(\Omega_0 + \Omega_{\Lambda} = 1)$, we have used an approximation given by Kitayama & Suto (1996). Here Ω_f is the value of the mass density ratio Ω at the redshift of formation,

$$\Omega_f = \frac{\Omega_0 (1+z)^3}{\Omega_0 (1+z)^3 + \Omega_\Lambda}.$$
 (7)

In this model the growth factor can be written as
$$D(x) = \frac{(x^3 + 2)^{1/2}}{x^{3/2}} \int_{x_0}^x x^{3/2} (x^3 + 2)^{-3/2} dx \qquad (8)$$

(Peebles 1980, eqn. 13.6) where $x_0 \equiv \left(\frac{2\Omega_{\Lambda}}{\Omega_0}\right)^{1/3}$ and x = $x_0/(1+z)$.

Figure 1 shows how the cluster abundance evolves with redshift for the three cosmologies under consideration. For each model we plot the integrated number density of clusters at each redshift, which is simply the integral of equation (3) over all masses $M \geq 8 \times 10^{14} \, h^{-1} \, M_{\odot}$. The mass plotted here is the virial mass, which is the mass within the virial radius. The closed model shows the strongest evolution, followed by the flat model, with the open model showing the weakest evolution, as expected (e.g., Bahcall & Fan 1998).

2.2. Comparison to Observed X-ray Luminosity Function

As a check on these models, we have estimated the resulting X-ray luminosity function of clusters at the present epoch. To convert the predicted mass function of clusters to an X-ray luminosity function, we first determine the temperatures of the gas in clusters using the observed mass-temperature relationship (Evrard, Metzler, & Navarro 1996; Horner, Mushotzky, & Scharf 1999)

$$M = c_0 \times 10^{13} h^{-1} \left(\frac{T_X}{T_m}\right)^{c_1} M_{\odot},$$
 (9)

where $T_m \equiv 1 \text{ keV}$, $c_0 \approx 5$, and $c_1 \approx 1.5$. Then, the X-ray luminosities L_X were calculated from the X-ray temperatures using the X-ray luminosity-temperature relationship (Arnaud & Evrard 1999)

$$L_X = b_0 \times 10^{44} \, h^{-2} \left(\frac{T_X}{T_l}\right)^{b_1} \,\mathrm{erg \, s^{-1}} \,,$$
 (10)

where T_X is the X-ray temperature, $T_l \equiv 6 \text{ keV}$ is a characteristic value used for scaling, $d_0 \approx 2.88$, and $d_1 \approx 2.88$. Here, L_X is the bolometric X-ray luminosity. Figure 2 shows the resulting differential luminosity function at the current epoch as predicted by PS for our three cosmolo-

For comparison, we overplot the observed local bolometric X-ray luminosity function from Ebeling et al. (1997),

$$\frac{dn}{dL_X} = a_0 \times 10^{-8} h^5 \exp(-L_X/L_X^*)
\times \left(\frac{L_X}{L_X^*}\right)^{-a_1} \text{Mpc}^{-3} \left(10^{44} \text{ erg s}^{-1}\right).$$
(11)

Here, $L_X^* \approx 9.3 \times 10^{44} \ \rm erg \ s^{-1}$ is a characteristic cluster X-ray luminosity, $a_0 \approx 2.64$, and $a_1 \approx 1.84$. The model is in reasonable agreement with the observations.

3. PREDICTED EMISSION FROM CLUSTERS OF GALAXIES

As discussed in § 1, EUV and very soft X-ray emission has been detected from a number of clusters of galaxies. Although it is not yet certain how common this emission is, we will assume that it is a general feature of clusters. As we noted in \S 1, this implies that our results are upper limits on the extragalactic EUV background due to clusters, if EUV emission is not a common phenomena. While the mechanism for this emission is still under debate, inverse Compton (IC) scattering of the cosmic microwave background (CMB) by cosmic-ray electrons seems to be a very strong candidate (Hwang 1997; Bowyer & Berghöfer 1998; Enßlin & Biermann 1998; Sarazin & Lieu 1998). For the purposes of this analysis, we will assume that IC scattering is the dominant source of EUV radiation from clusters. However, we will normalize our models to the observed EUV flux of the Coma cluster; the IC model will be used to scale this flux to other cluster masses and redshifts.

The IC luminosity from an individual cluster is given by

$$L_{IC} = \frac{4}{3} \frac{\sigma_T}{m_e c} \langle \gamma \rangle U_{CMB} E_{CR}, \tag{12}$$

where U_{CMB} is the energy density in the CMB, E_{CR} is the total energy in cosmic-ray electrons in the cluster, and $\langle \gamma \rangle$ is the average Lorentz factor of the cosmic-rays:

$$\langle \gamma \rangle \equiv \frac{\int n_{CR}(\gamma) \gamma^2 d\gamma}{\int n_{CR}(\gamma) \gamma d\gamma},\tag{13}$$

where $n_{CR}(\gamma)d\gamma$ is the number density of cosmic-ray electrons with Lorentz factors between γ and $\gamma + d\gamma$. The EUVE observations of clusters suggest that $\langle \gamma \rangle \approx 300$ (for a Hubble constant of 50 km s⁻¹ Mpc⁻¹; Sarazin & Lieu 1998). One expects that this value will correspond to electrons whose lifetimes are similar to the age of the cluster (Sarazin 1999), which implies that $\langle \gamma \rangle \propto h$. Thus, we assume that

$$\langle \gamma \rangle = 600 \, h \tag{14}$$

(Sarazin & Lieu 1998). The energy density in the CMB is well determined by observations, $U_{CMB} = 4 \sigma_T T_{CMB}^4 / c =$

 $4.20 \times 10^{-13} (1+z)^4 \text{ ergs cm}^{-3}$, where T_{CMB} is the temperature of the CMB, $T_{CMB} = 2.73 (1+z) \text{ K}$.

The observed EUV luminosities of clusters imply that the total energies of cosmic ray electrons are $E_{CR} \sim 10^{62}$ ergs (for a Hubble constant of 50 km s⁻¹ Mpc⁻¹; Sarazin & Lieu 1998). These values are typically 1–10% of the thermal energy content of the intracluster gas, E_{gas} . The observed values of E_{gas} scale as $E_{gas} \propto h^{-5/2}$. The thermal energy content of the intracluster gas is the result of shock heating, where the shocks might include cluster merger shocks, overall accretion shocks, and shocks produced by galaxy winds (Sarazin 2000). These shocks all have velocities of $\sim 1000 \text{ km s}^{-1}$. Supernova remnants and other diffuse astrophysical shocks with similar velocities accelerate relativistic particles, and the radio properties of supernova remnants imply that $\sim 3\%$ of the shock energy goes into accelerating relativistic electrons (e.g., Blandford & Eichler 1987). Since both the relativistic electrons and the thermal energy in the intracluster gas arise from the same shocks, it seems reasonable to assume that the energy which is injected in relativistic electrons is proportional to the thermal energy content of the ICM. Thus, we will assume that

$$E_{CR} = f_{CR} E_{gas} \,. \tag{15}$$

We adopt a fixed value for f_{CR} which is determined by the observed EUV flux from the Coma cluster, which is the best observed rich cluster. To determine f_{CR} , we apply the Galactic absorption and redshift appropriate to Coma to our adopted spectral model (see Figure 3 below). Then, the resulting spectrum was convolved with the EUVE effective area to give the expected count rate. This was compared to the observed values of the EUVEcount rate (Lieu et al. 1996a; Bowyer & Berghöfer 1998; Bowyer et al. 1999) which range over a factor of about two. The model spectrum was renormalized to give the observed count rate, and the total cosmic ray energy E_{CR} was determined. The ROSAT X-ray observations of Coma were used to determine the total gas mass within the projected radius of the EUV observations (e.g., Mohr, Mathiesen, & Evrard 1999). The corresponding thermal energy content of the gas E_{gas} was derived. Finally, E_{CR} and E_{gas} for Coma were compared to give f_{CR} (eq. 15). The values were $f_{CR} = (0.014 - 0.031)h^{-1/2}$, corresponding to the range in observed count rates for Coma. We adopt the value $f_{CR} = 0.02 \, h^{-1/2}$. This is consistent with the reported fluxes of other clusters (Sarazin & Lieu 1998). For any individual cluster, it is likely that E_{CR} and f_{CR} will depend on its dynamical history, but we assume that on average there is a simple relationship between the thermal energy in the gas and the energy in relativistic particles.

The ICM thermal energy is given by

$$E_{gas} = \frac{3}{2} \frac{kT}{\mu m_p} M_{gas} \,, \tag{16}$$

where T is the average temperature of the ICM, $\mu=0.61$ is the mean mass per particle in units of the proton mass m_p , and M_{gas} is the mass of the ICM. There are a number of arguments which suggest that a portion of the thermal energy of the ICM may have come from non-gravitational effects which probably occurred before the clusters formed (e.g., Kaiser 1991; Cavaliere, Menci, & Tozzi 1997). Even if this heating involved shocks, it is unlikely that primary

electrons accelerated in such shocks survive to the present epoch (Sarazin 1999). Thus, we will determine the gas temperature in our model clusters using a theoretical relationship based on purely gravitational effects, which is consistent with the PS formulation and with numerical hydrodynamical simulations of cluster formation from large scale structure. We choose the mass-temperature relationship

$$kT = 1.39 f_T \left(\frac{M}{10^{15} M_{\odot}}\right)^{2/3}$$
 $\times \left[h^2 \Delta_c E(z)^2\right]^{1/3} \text{ keV}, \qquad (17)$

where $f_T \approx 0.8$ is a normalization factor (Bryan & Norman 1998). The quantity E(z) is defined as $E(z)^2 \equiv \Omega_0(1+z)^3 + \Omega_R(1+z)^2 + \Omega_\Lambda$, where $\Omega_R \equiv 1/(H_0R)^2$ where R is the current radius of curvature of space. Δ_c represents the mean density of the cluster divided by the critical density at a given redshift. Fits for this parameter are given by Bryan & Norman (1998) for the relevant cosmological models:

$$\Delta_c = \begin{cases} 18\pi^2 + 82x - 39x^2 & (\Omega_R = 0) \\ 18\pi^2 + 60x - 32x^2 & (\Omega_\Lambda = 0) \end{cases}$$
 (18)

where $x \equiv [\Omega_0(1+z)^3/E(z)^2] - 1$. Note that $\Omega_R = 0$ is a consequence of the flat model (flat space has an infinite curvature). When $\Omega_0 = 1$, x = 0, giving $\Delta_c = 18\pi^2$.

Finally, we need to determine the total gas mass M_{gas} of our clusters. X-ray observations indicate that the gas fraction in cluster is fairly constant for rich clusters, with a value of $\approx 22\%$ (for a Hubble constant of 50 km s⁻¹ Mpc⁻¹; e.g., Arnaud & Evrard 1999). Thus, we assume that

$$M_{gas} = f_{gas} M, (19)$$

with $f_{gas} = 0.07 h^{-3/2}$.

Using equations (12)-(19), we calculate the average IC luminosity L_{IC} of a cluster of a given total mass M. For individual clusters, one expects the spectrum of IC EUV emission will depend on the history of particle acceleration in the cluster (Sarazin 1999). For this study, we adopt a "typical" IC EUV spectrum, since we intend to average over an ensemble of clusters to determine the cluster contribution to the EUV background. Specifically, we assume the spectral shape given for Model 11 in Sarazin (1999). This adopted model spectrum L_{ν} (model) is shown in Figure 3, where L_{ν} is the luminosity per unit frequency ν . This particular model spectrum has a total IC luminosity of $L_{IC}(\text{model}) = 2.86 \times 10^{44} \text{ ergs s}^{-1}$. The normalization of the spectrum of each model cluster is scaled to give the correct value of L_{IC} for that cluster. At redshifts z > 0, the spectrum is blue shifted due to the increase in the temperature of the CMB. Thus, the spectrum of emission of a cluster with total mass M at redshift z is given by

$$L_{IC}(M, z, \nu) = L_{IC}(M, z) \frac{L_{\nu/(1+z)}(\text{model})}{(1+z)L_{IC}(\text{model})}.$$
 (20)

3.1. The Diffuse Radiation Field

The total emissivity of cluster IC emission at any given redshift is found by integrating the emission due to clusters of a given total mass M (eq. 20) over the PS mass function (eq. 3):

$$\epsilon(\nu, z) = \int L_{IC}(M, z, \nu) n(M, z) dM. \qquad (21)$$

The total emissivity over all frequencies is just

$$\epsilon_{tot}(z) = \int \epsilon(\nu, z) \, d\nu = \int L_{IC}(M, z) \, n(M, z) \, dM \,. \tag{22}$$

The equation of radiative transfer for the emission gives a mean intensity for the radiation field at an observed redshift z_o and observed frequency ν_o of (Haardt & Madau 1996)

$$J(\nu_o, z_o) = \frac{1}{4\pi} \int_{z_o}^{\infty} dz \, \frac{dl}{dz} \frac{(1+z_o)^3}{(1+z)^3} \times \epsilon(\nu, z) \, e^{-\tau_{eff}(\nu_o, z_o, z)} \,.$$
(23)

Here, dl/dz is the line element in a Friedmann cosmology, given by

$$\frac{dl}{dz} = \frac{c}{H_0} (1+z)^{-1} \times \left[\Omega_0 (1+z)^3 + \Omega_R (1+z)^2 + \Omega_\Lambda \right]^{-1/2} . \quad (24)$$

The quantity $\tau_{eff}(\nu_o, z_n, z)$ gives the effective optical depth of the intergalactic medium (IGM) at the observed frequency between z_o and z. We can simplify equation (23) by noting that the energy density in the CMB, which is present in our expression for $\epsilon(z)$ through the L_{IC} term, goes as $(1+z)^4/(1+z_o)^4$. When we consider the emissivity per unit frequency $\epsilon(\nu,z)$, we get another factor of $(1+z_o)/(1+z)$ due to the redshift applied at each frequency. Multiplying these factors together gives us a net factor of $(1+z)^3/(1+z_o)^3$, which directly cancels the redshift term in equation (23). We can therefore rewrite this equation as

$$J(\nu_o, z_o) = \frac{1}{4\pi} \int_{z_o}^{\infty} dz \, \frac{dl}{dz} \, \epsilon(\nu_o, z) \, e^{-\tau_{eff}(\nu_o, z_o, z)} \,, \quad (25)$$

where $\epsilon(\nu_o, z)$ is defined as the emissivity for a cluster population at a redshift z calculated as though it were actually located at redshift z_o .

The opacity of the IGM is mainly due to the effective column density of the less ionized clouds (such as $\text{Ly}\alpha$ clouds). In determining the optical depth of the IGM, we closely follow the treatment in Haardt & Madau (1996). They write the optical depth of the IGM as

$$\tau_{eff}(\nu_o, z_o, z) = \int_{z_o}^{z} dz' \int_0^{\infty} dN_{HI} \frac{\partial^2 N}{\partial N_{HI} \partial z'} \times \left[1 - e^{-\tau(N_{HI}, z', \nu)} \right], \qquad (26)$$

where N_{HI} is the column density of neutral hydrogen in a IGM cloud, and $(\partial^2 N/\partial N_{HI}\partial z')$ gives the number of clouds per unit H I column and per unit redshift z'. The quantity $\tau(N_{HI}, z', \nu)$ is the optical depth of a cloud with an H I column of N_{HI} at redshift z' for the frequency $\nu = \nu_o(1+z')/(1+z_o)$; this depends on the helium abundance and the ionization structure of the clouds; we adopt the abundances and ionization structures calculated in Haardt & Madau (1996). For the ionization, we use the approximation given in their equation (12), with η_{thin} taken from their Figure 7.

4. RESULTS

4.1. Models without IGM Absorption

We first calculate the diffuse radiation field neglecting IGM absorption ($\tau_{eff} = 0$ in eq. [23]). Here, we consider

only the values at the present epoch, $z_o=0$. We find the total mean intensity to be $1.0\times 10^{-10}~\rm ergs~cm^{-2}~s^{-1}~sr^{-1}$ for the open model, $9.0\times 10^{-11}~\rm ergs~cm^{-2}~s^{-1}~sr^{-1}$ for the flat model, and $4.7\times 10^{-11}~\rm ergs~cm^{-2}~s^{-1}~sr^{-1}$ for the closed model.

We have calculated the spectrum of the cluster EUV background at the present epoch, z=0, neglecting absorption for our three cosmological models. Results are plotted in Figure 4. The corresponding ionization rates have been determined by integrating each of these radiation fields over the ionization cross-sections of H I and He II. The results are $\zeta_H=1.8\times10^{-17},\,1.6\times10^{-17},\,8.6\times10^{-18}$ and $\zeta_{HeII}=2.05\times10^{-18},\,1.8\times10^{-18},\,9.7\times10^{-19}\,\mathrm{s}^{-1}$ for the open, flat, and closed cosmological models, respectively.

4.2. Models with IGM Absorption

Next, we calculate models including the opacity of the IGM, following the treatment of Haardt & Madau (1996).

4.2.1. Present Epoch Diffuse Radiation

We have first calculated the values for the diffuse cluster IC radiation field at the present epoch, $z_o = 0$. We find the total mean intensity to be 9.0×10^{-11} ergs cm⁻² s⁻¹ sr⁻¹ for the open model, 8.2×10^{-11} ergs cm⁻² sr⁻¹ for the flat model, and 4.5×10^{-11} ergs cm⁻² sr⁻¹ for the closed model. We note that the numbers are only slightly smaller than the values ignoring absorption (§ 4.1 above). Unlike the ionizing background from quasars, most of the diffuse emission from clusters is produced at relatively small redshifts (§ 4.2.2 below), where the IGM opacity is low.

The predicted spectrum of the EUV background from clusters at the present epoch $z_o = 0$ is shown in Figure 5 for each of our three cosmological models. The "bumps" in these curves are due to absorption by H I and He II. Clearly, absorption has only a small effect on the spectrum (compare with Figure 4). The present day ionization rates for cluster EUV models with IGM absorption are $\zeta_H = 1.6 \times 10^{-17}$, 1.5×10^{-17} , 8.2×10^{-18} and $\zeta_{HeII} = 1.6 \times 10^{-18}$, 1.4×10^{-18} , 8.5×10^{-19} s⁻¹ for the open, flat, and closed cosmological models, respectively. Ionization rates from QSOs are given below for comparison (§ 4.2.2).

Figure 6 compares the predicted contributions of clusters and quasars to the diffuse EUV background at $z_o=0$ for the open cosmological model. The quasar results are taken from Haardt & Madau (1996), Figure 5a. A comparison of the two curves shows that the contribution to the EUV background from clusters is $<\frac{1}{2}\%$ of that of quasars. Thus, while clusters do make a contribution to the EUV background at the present epoch, the predominant source is due to AGN.

4.2.2. Redshift Evolution

The spectrum of the diffuse radiation field due to cluster IC EUV is plotted as observed at redshifts of $z_o = 0$, 0.5, and 1.0 for the open cosmological model in Figure 7. Models were calculated for higher redshifts ($z \ge 1.5$), but the values much smaller than those shown. This figure clearly shows that the intensity of the EUV background from clusters decreases strongly with increasing redshift,

which means that the largest contribution to the EUV background from clusters occurs at the current epoch. On the other hand, the predicted intensity of the diffuse UV radiation field due to quasars increases with increasing redshifts out to $z_o \sim 3$. (Haardt & Madau 1996, Figure 5). Thus, the fractional contribution to the EUV background from clusters as compared to quasars also decreases strongly with redshift. This is because the abundance of rich clusters increases with time due to gravitational mergers of smaller systems, while quasars were most abundant in the early universe (at $z \gtrsim 2$).

The ionization rate due to cluster EUV also decreases rapidly with increasing redshift. We find rates of $\zeta_H=1.6\times 10^{-17},\ 2.0\times 10^{-18},\ 1.2\times 10^{-19},\ 3.9\times 10^{-21}\ {\rm s}^{-1}$ for H I and $\zeta_{HeII}=1.6\times 10^{-18},\ 2.1\times 10^{-19},\ 1.3\times 10^{-20},\ 4.7\times 10^{-22}\ {\rm s}^{-1}$ for He II at $z_o=0,\ 0.5,\ 1.0,\ {\rm and}\ 1.5,\ {\rm respectively},\ {\rm for}$ the open cosmological model. To compare these results with those from QSOs, we use the results given by Haardt & Madau (1996, Fig. 6) for an open cosmological model with $q_0=0.1,\ {\rm which}\ {\rm give}\ \zeta_H=4.1\times 10^{-14},\ 1.6\times 10^{-13},\ 4.5\times 10^{-13},\ 9.3\times 10^{-13}\ {\rm s}^{-1}$ for H I and $\zeta_{HeII}=4.1\times 10^{-16},\ 1.6\times 10^{-15},\ 4.4\times 10^{-15},\ 9.0\times 10^{-15}$ s⁻¹ for He II at $z_o=0,\ 0.5,\ 1.0,\ {\rm and}\ 1.5,\ {\rm respectively}.$ In general, the ionization rates due to cluster EUV are <1% of those due to QSOs. The largest contribution is for the He II ionization rate at z=0, where the cluster EUV gives $\sim 0.4\%$ of the quasar rate.

5. CONCLUSION

Observations with EUVE indicate that some clusters of galaxies are luminous sources of extreme ultraviolet (EUV) radiation. In order to limit the contribution of EUV emis-

sion from clusters to the extragalactic background, we have assumed that this emission is a common feature of clusters. A promising theory for this emission is that it is due to IC scattering of the Cosmic Microwave Background photons by relativistic electrons. We have given a simple model for the average EUV luminosity expected from clusters based on this theory. We summed this emission over clusters of varying mass at different redshifts, using the Press-Schechter formalism to determine the mass function of clusters as a function of redshift. We determined the amount of background radiation produced by clusters through EUV IC emission. The total mean intensity, spectrum, and the ionization rates for H I and He II were determined at present and at a variety of redshifts. Because clusters form by the merger of smaller subclusters and the abundance of massive clusters increases with time, the amount of EUV background radiation should be larger at present than in the past. We compared our results to the ionizing background expected from quasars. We find that while clusters do contribute a significant EUV background, it is less than a percent of that expected from quasars. Of course, this last conclusion is strengthened if EUV emission is not a general feature of clusters.

We thank Avi Loeb and Ue-Li Pen for a useful conversation. Support for this work was provided by the National Aeronautics and Space Administration through Chandra Award Number GO0-1019X issued by the Chandra X-ray Observatory Center, which is operated by the Smithsonian Astrophysical Observatory for and on behalf of NASA under contract NAS8-39073.

REFERENCES

Arabadjis, J. S., & Bregman, J. N. 1999, ApJ, 514, 607
Arnaud, M. 2000, in Constructing the Universe with Clusters of Galaxies, ed. F. Durret, & D. Gerbal, in press
Arnaud, M., & Evrard, A. E. 1999, MNRAS, 305, 631
Atoyan, A. M., & Völk, H. J. 2000, ApJ, 535, 45
Bahcall, N. A., & Fan, X. 1998, ApJ, 504, 1
Berghöfer, T. W., Bowyer, S., & Korpela, E. J. 2000, ApJ, 535, 615
Blandford, R. D., & Eichler, D. 1987, Phys. Rep., 154, 1
Bowyer, S. 2000, private communication
Bowyer, S., & Berghöfer, T. W. 1998, ApJ, 506, 502
Bowyer, S., Berghöfer, T. W., 1998, ApJ, 506, 502
Bowyer, S., Lieu, R., & Mittaz, J. P. 1998, in The Hot Universe:
Proc. IAU Symp. 188. ed. K. Koyama, S. Kitamoto, & M. Itoh.
(Dordrecht: Kluwer), 185
Bryan, G. L., & Norman, M. L. 1998, ApJ, 495, 80
Cavaliere, A., Menci, N., & Tozzi, P. 1997, ApJ, 484, L21
Ebeling, H., Edge, A. C., Fabian, A. C., Allen, S. W., Crawford, C. S., & Böhringer, H. 1997, ApJ, 479, L101
Enßlin, T. A., & Biermann, P. L. 1998, A&A, 330, 90
Evrard, A. E., Metzler, C. A., & Navarro, J. F. 1996, ApJ, 469, 494
Fabian, A. C. 1996, Science, 271, 1244
Feretti, L. 1999, in Diffuse Thermal and Relativistic Plasma in Galaxy Clusters, ed. H. Böringer, L. Feretti, & P. Schuecker (Garching: MPE Report 271), 1
Haardt, F., & Madau, P. 1996, ApJ, 461, 20
Horner, D. J., Mushotzky, R. F., & Scharf, C. A. 1999, ApJ, 520, 78
Hwang, C.-Y. 1997, Science, 278, 1917

Kaastra, J. S., Lieu, R., Mittaz, J. P. D., Bleeker, J. A. M., Mewe, R., Colafrancesco, S., & Lockman, F. J. 1999, ApJ, 519, L119 Kaiser, N. 1991, ApJ, 383, 104 Kitayama, T., & Suto, Y. 1996, ApJ, 469, 480 Lacey, C., & Cole, S. 1993, MNRAS, 262, 627 Lieu, R., Bonamente, M., & Mittaz, J. P. D. 1999a, ApJ, 517, L91 Lieu, R., Bonamente, M., Mittaz, J. P. D., Durret, F., Dos Santos, S., & Kaastra, J. S. 1999b, ApJ, 527, L77

Lieu, R., Mittaz, J. P. D., Bowyer, S., Breen, J. O., Murphy, E. M., Lockman, F. J., & Hwang, C.-Y. 1996a, Science, 274, 1335

Lieu, R., Mittaz, J. P. D., Bowyer, S., Lockman, F. J., Hwang, C.-Y., & Schmitt, J. H. M. M. 1996b, ApJ, 458, L5 Lieu, R., Mittaz, J. P. D., Bowyer, S., Schmitt, J. H. M. M., & Lewis J. 1996c, in Astrophysics in the Extreme Ultraviolet: Proc. IAU Symp. 152, ed. S. Bowyer, & R. F. Malina (Dordrecht: Kluwer), Mittaz, J. P. D., Lieu, R., & Lockman, F. J. 1998, ApJ, 498, L17 Mohr, J. J., Mathiesen, B., & Evrard, A. E. 1999, ApJ, 517, 627 Peebles P. J. E. 1980, The Large-Scale Structure of the Universe (Princeton: Princeton Univ. Press) Prèss, W. H., & Schechter, P. 1974, ApJ, 187, 425 Sarazin, C. L. 1999, ApJ, 520, 529 Sarazin, C. L. 2000, in Large-Scale Structure in the X-ray Universe, ed. M. Plionis & I. Georgantopoulos (Biarritz: Atlantisciences), 81 (astro-ph/9911439) Sarazin, C. L., & Lieu, R. 1998, ApJ, 494, L177 Takizawa, M., & Naito, T. 2000, ApJ, 535, 586 Viana, P. T. P., & Liddle, A. R. 1999, preprint (astro-ph/9902245)

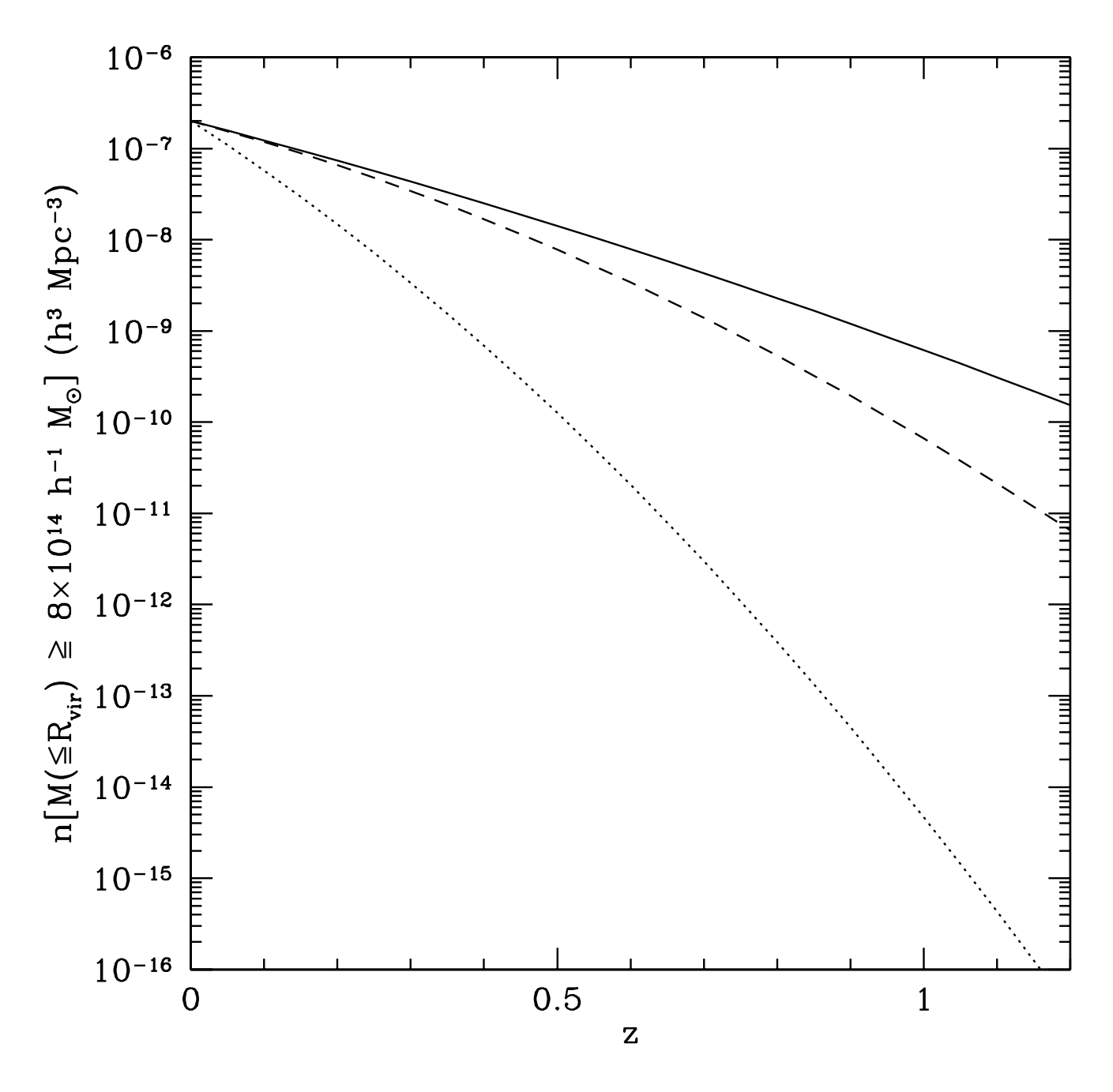


FIG. 1.— The evolution of the abundance of clusters with redshift z for three distinct cosmologies. Only clusters with mass $M \geq 8 \times 10^{14} \, h^{-1} \, M_{\odot}$ within their virial radius R_{vir} are considered. The solid curve represents an open Universe ($\Omega_0 = 0.3$, $\Omega_{\Lambda} = 0$), the dashed curve a flat Universe ($\Omega_0 = 0.3$, $\Omega_{\Lambda} = 0.7$), and the dotted curve a closed Universe ($\Omega_0 = 1.0$, $\Omega_{\Lambda} = 0$).

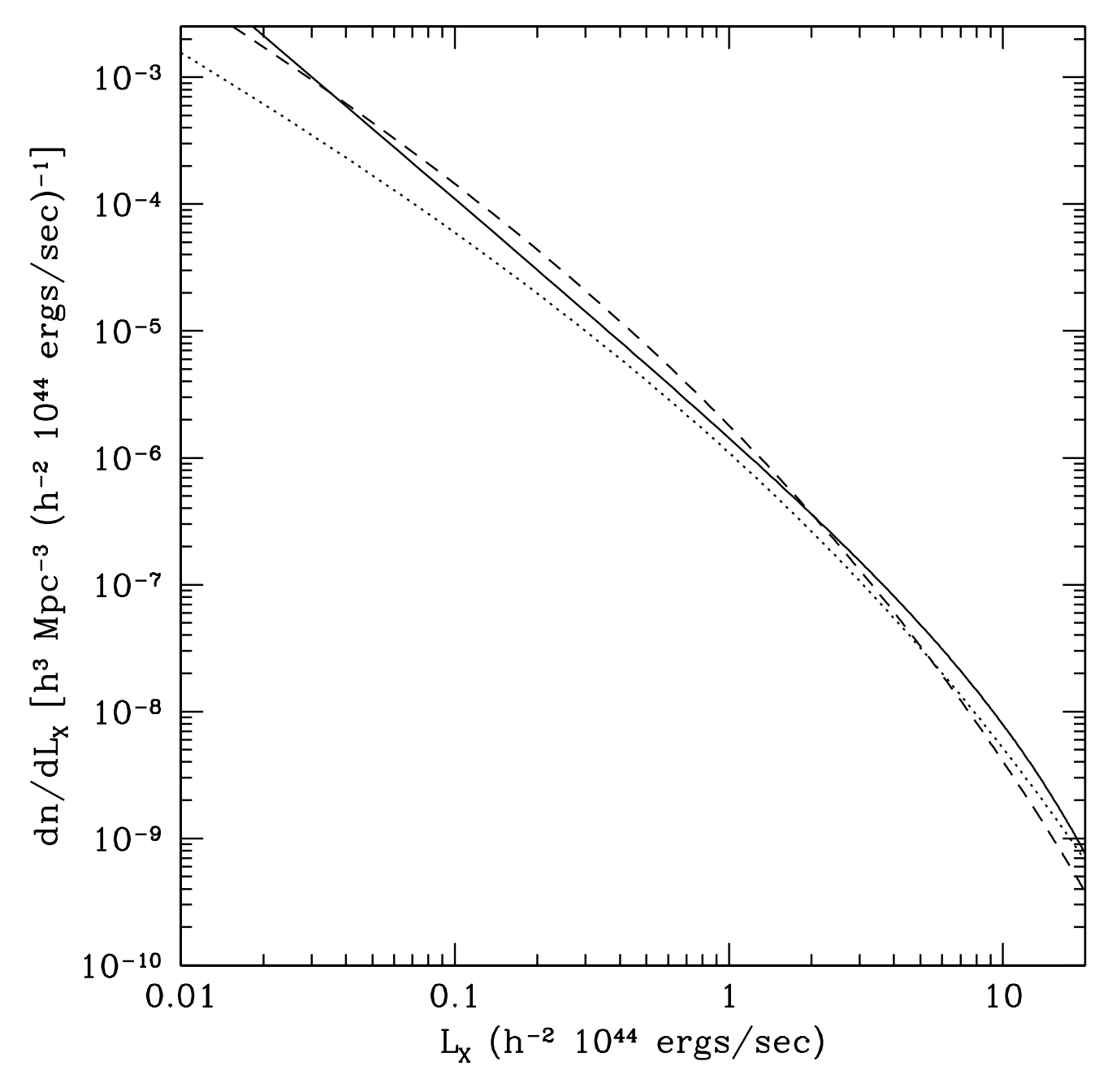


Fig. 2.— The present day cluster bolometric X-ray luminosity function. The solid curve is the observed luminosity function (Ebeling et al. 1997). The dashed curve shows the predicted luminosity function for a closed Universe ($\Omega_0 = 1$, $\Omega_{\Lambda} = 0$), while the dotted curve shows the predicted luminosity function for an open Universe ($\Omega_0 = 0.3$, $\Omega_{\Lambda} = 0$). The flat Universe is omitted here for clarity since the predicted curve essentially matches the predicted curve for the open Universe.

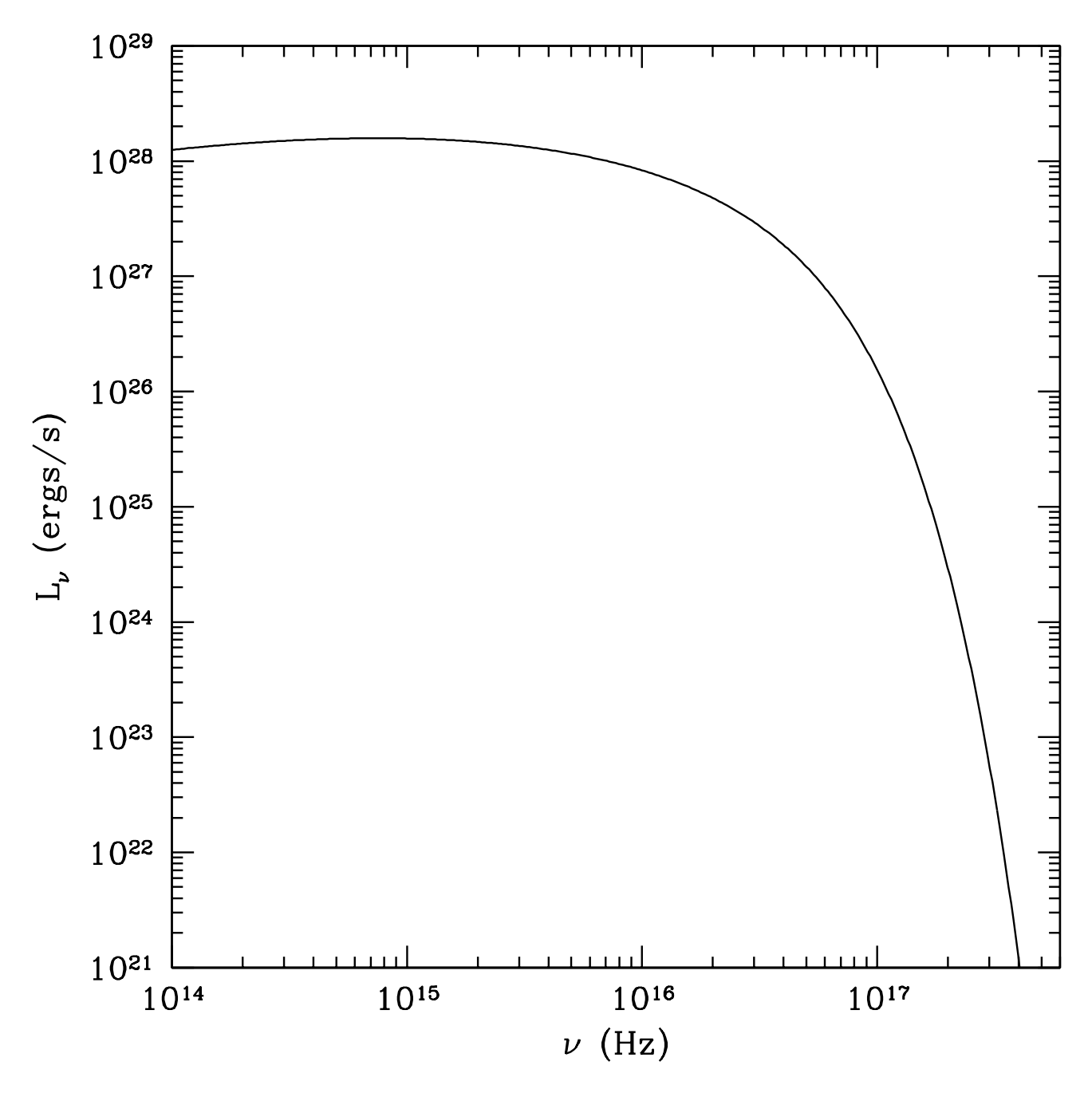


Fig. 3.— The adopted IC EUV spectrum for our clusters, which is the spectrum of Model 11 in Sarazin (1999). Here, L_{ν} is the luminosity per unit frequency ν . This model has a total IC luminosity of $L_{IC}=2.86\times10^{44}~{\rm ergs~s^{-1}}$. The normalization of the spectrum of each model cluster is scaled to give the correct value of L_{IC} for that cluster.

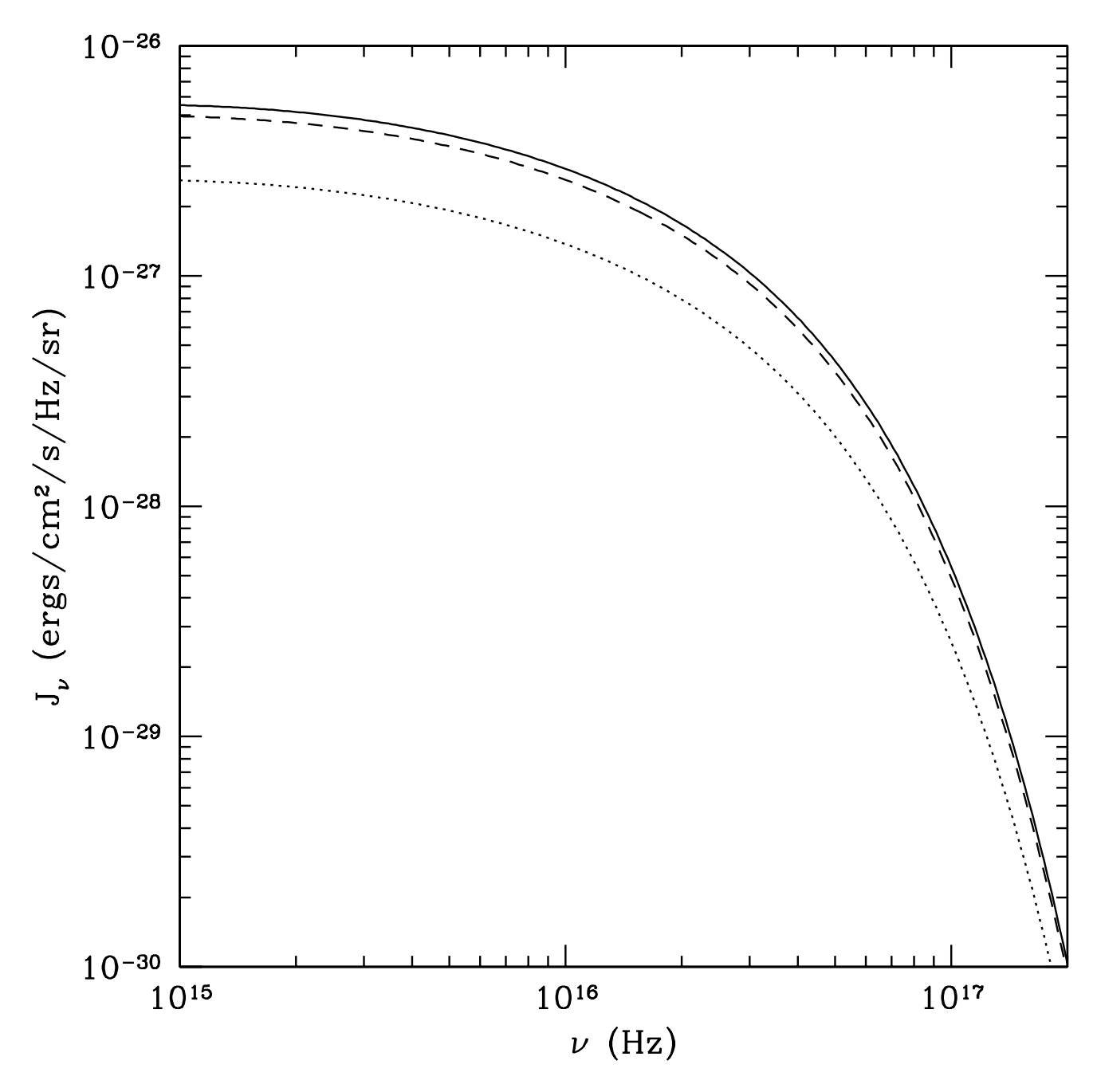


Fig. 4.— The mean specific intensity of the EUV background expected from clusters at the current epoch for three distinct cosmologies. The solid curve represents an open Universe ($\Omega_0=0.3$, $\Omega_{\Lambda}=0$), the dashed curve a flat Universe ($\Omega_0=0.3$, $\Omega_{\Lambda}=0.7$), and the dotted curve a closed Universe ($\Omega_0=1.0$, $\Omega_{\Lambda}=0$). Absorption effects are ignored.

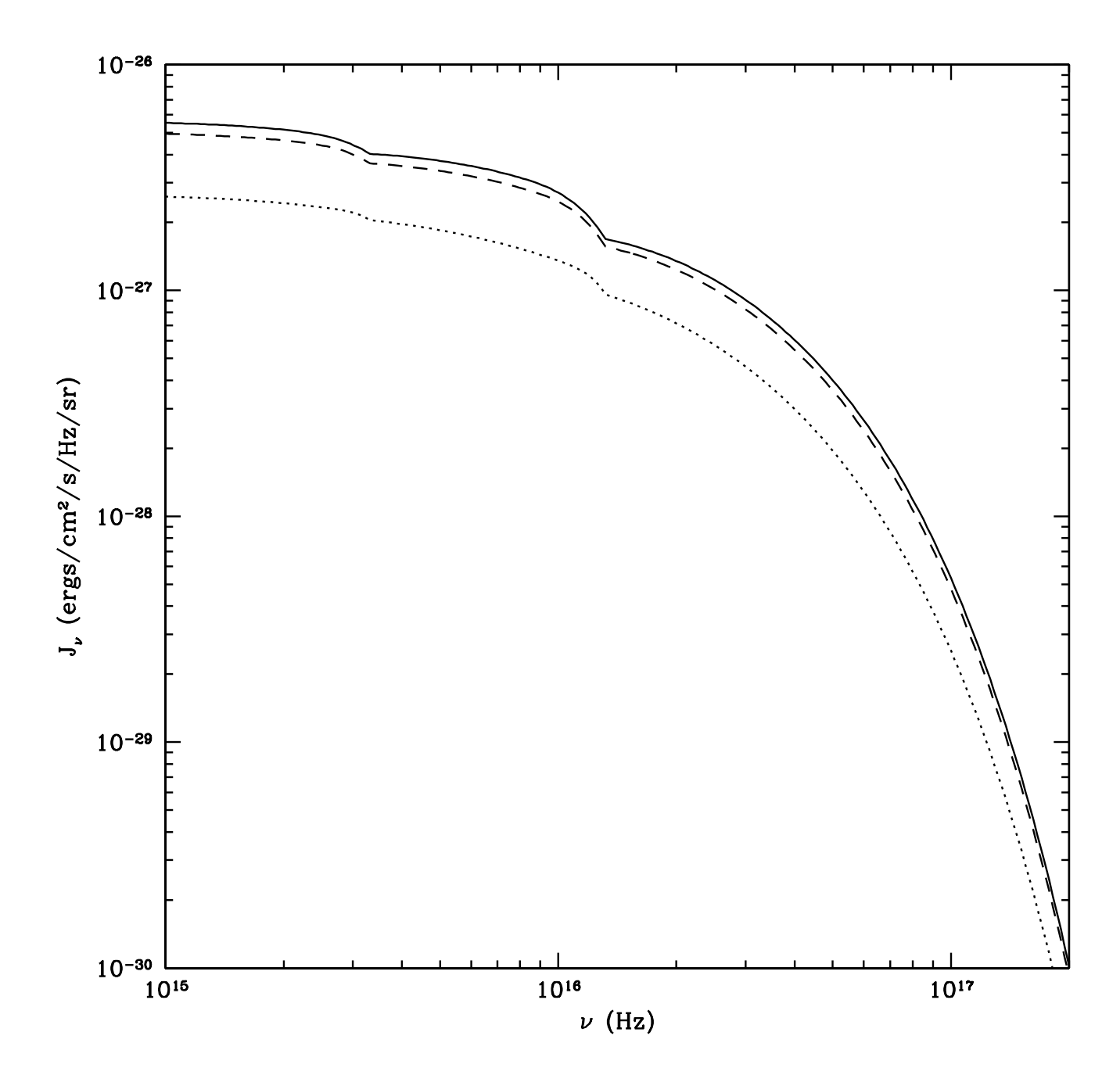


Fig. 5.— The mean specific intensity of the EUV background predicted by models including IGM absorption by H I and He II. The notation is the same as in Figure 4.

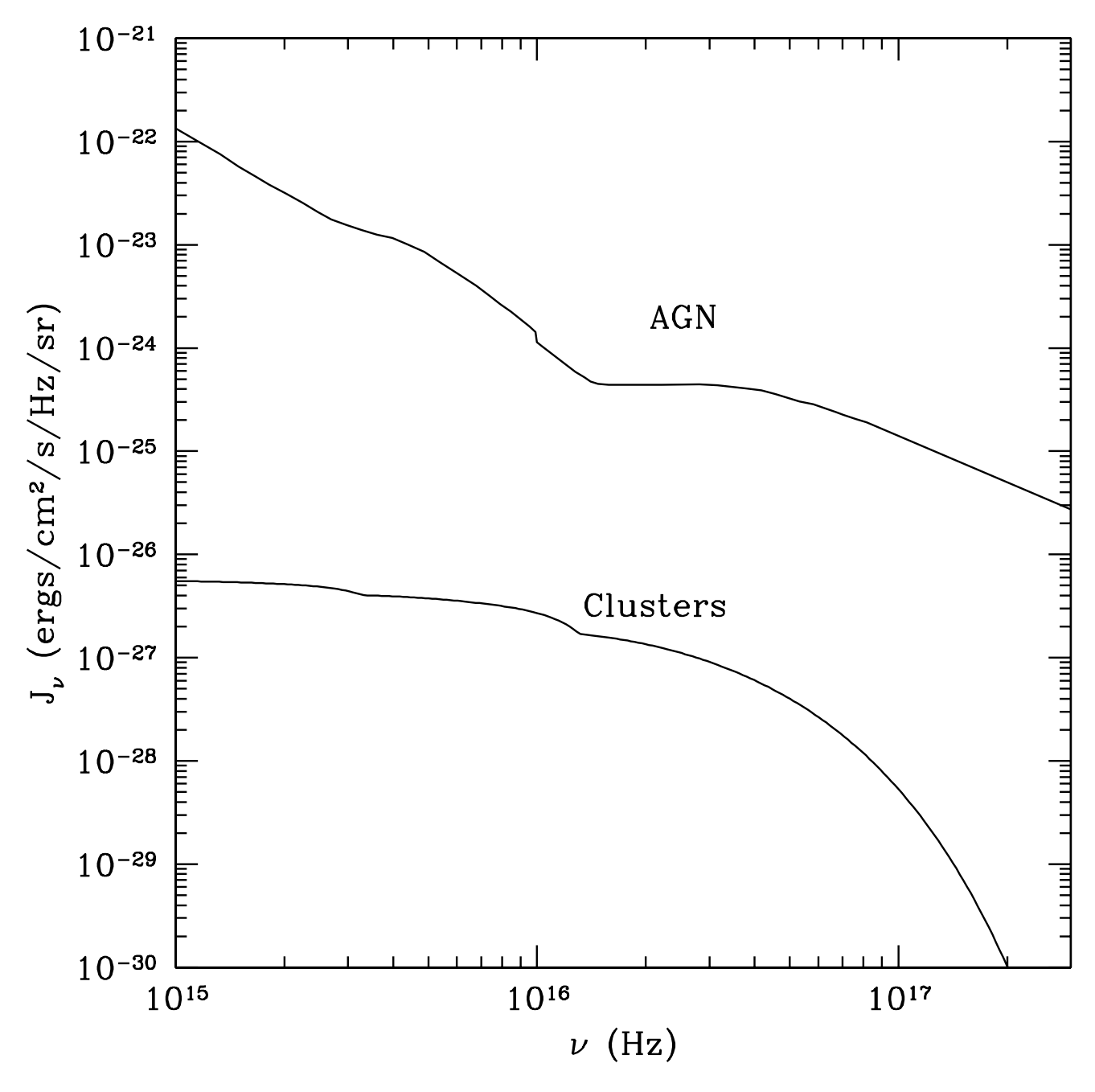


Fig. 6.— The predicted mean specific intensity of the EUV background at z=0 for an open Universe. The curve labeled "Clusters" shows the contribution from clusters while the curve labeled "AGN" shows the contribution from quasars.

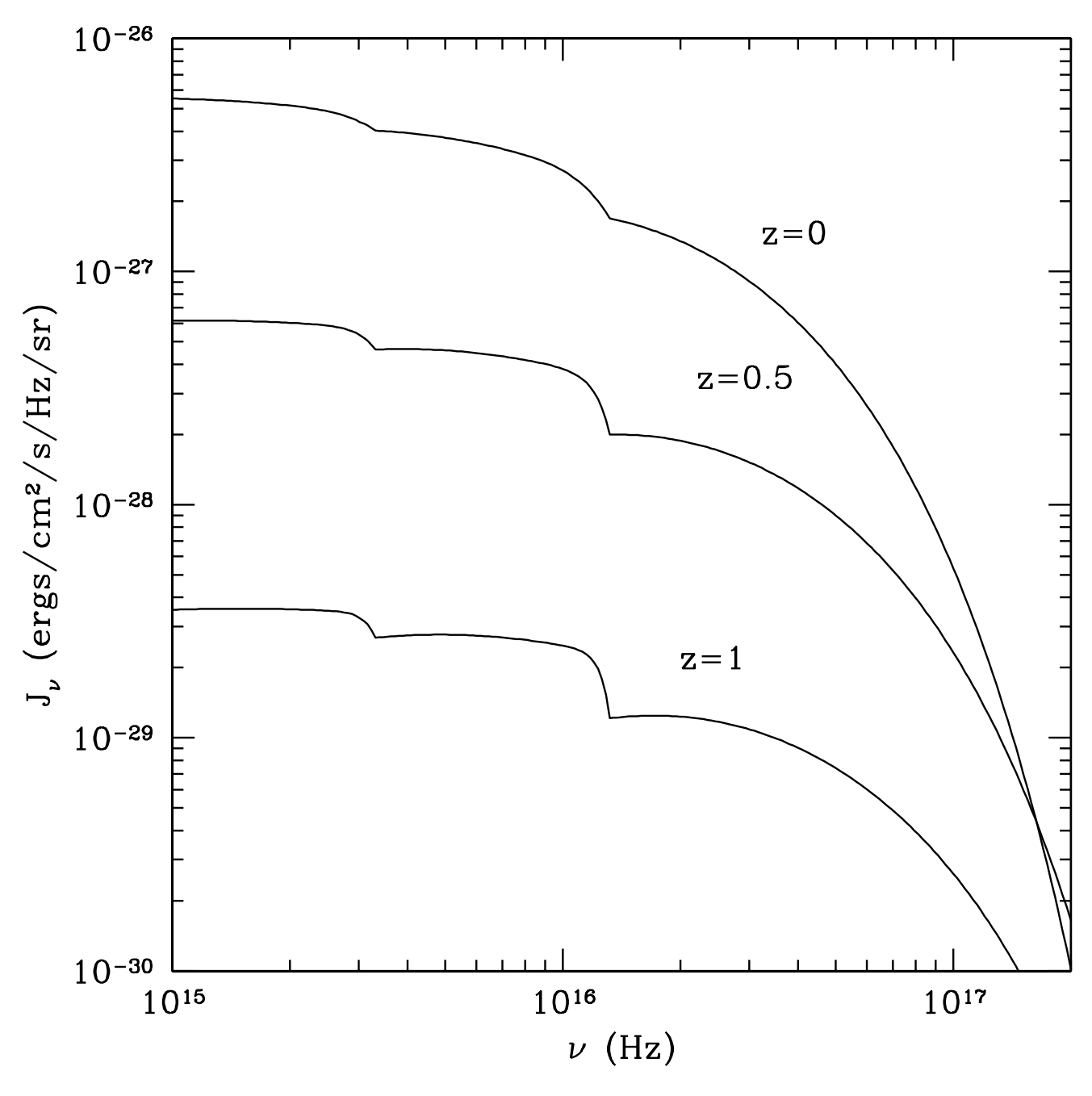


Fig. 7.— The spectrum of the diffuse EUV background from clusters as observed at redshifts z=0, z=0.5, and z=1 for the open cosmological model including IGM absorption.